An Equivalent Circuit Model of FSS-Based Metamaterial Absorber Using Coupled Line Theory

Saptarshi Ghosh, *Student Member, IEEE*, and Kumar Vaibhav Srivastava, *Senior Member, IEEE*

***Abstract*—An equivalent circuit model of an ultra-thin metamaterial absorber comprising a square-ring-shaped frequency selective surface (FSS) is presented. The model can be considered as series RLC resonators connected in parallel with coupling capacitance and short-circuited transmission line. The even- and odd-mode couplings have been incorporated to accurately determine the lumped parameters as well as the absorption frequency of the absorber structure. The effects of substrate thickness and dielectric permittivity variation on the lumped parameters and full width at half-maximum (FWHM) bandwidth are investigated based on the proposed model. The absorber has been fabricated, and close matching among the calculated, simulated, and measured results has been observed.**

***Index Terms*—Equivalent circuit, frequency selective surface, lumped parameter, metamaterial absorber.**

I. Introduction

RECENTLY, frequency selective surfaces (FSSs) have drawn significant research interests due to their variety of electromagnetic applications, such as electromagnetic absorber, filters, and antennas [1]–[3]. For analyzing the electromagnetic behavior of FSSs, several mathematical approaches (FEM, FDTD, MOM) are commonly employed [4], [5]. Despite their accuracy in analysis, these techniques require time-consuming simulations and do not allow the designer to have a good insight into the physics behind the structures. During the last few years, many researchers have tried to derive accurate formulas to suitably represent these surfaces. For simple shapes, analytical formulas have been derived simply by considering the average permittivity of the dielectrics on two sides of an FSS [6]. In other cases, transmission line theory has been used to explain the mechanism of the structures [7]. Some circuit models based on lumped circuit theory have been used to derive the element values, but they fail to explain any coupling effect among the neighboring periodic structures [8], [9]. Some circuit has modeled dielectric as capacitive impedance, but its value had not been calculated [10].

In this letter, a novel circuit model of the metamaterial absorber structure based on FSSs has been presented for the first time, which incorporates the coupling theory with the periodic array structures. Depending on the surface current distribution in the FSSs, even- and odd-mode couplings among the unit cells have been considered in the proposed model. A single square-ring structure with grounded dielectric substrate has been selected as a metamaterial absorber, whose absorption frequency has been accurately determined. The effects of the FSS shape (in terms of the length, width, permittivity, thickness, and unit cell period) on the absorption frequency are calculated and compared to the simulated responses. In particular, this proposed circuit model provides in-depth physical insight into the effects of lumped parameters for different substrate thicknesses and dielectric permittivity values based on the model. Afterwards, the full width at half-maximum (FWHM) bandwidth of the absorber structure has also been analyzed. The structure has been fabricated, and absorption frequency is experimentally measured, which is in good agreement with the simulated as well as analytical results. Finally, the effects of the substrate thickness variation for different widths of the square ring have been studied, thus validating the modelization technique for FSS-based microwave absorber structures.

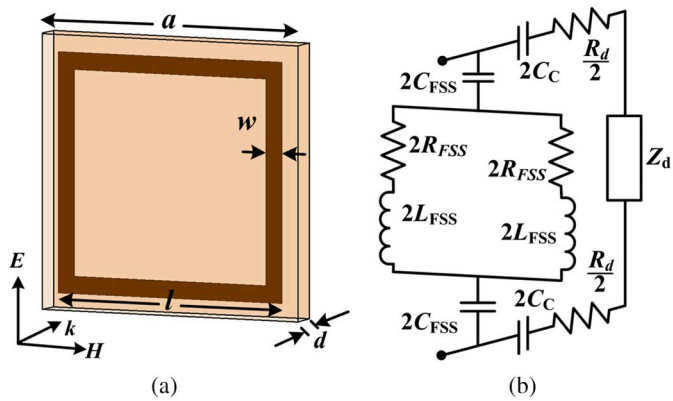

Fig. 1. (a) Perspective view and (b) equivalent circuit of the unit cell of the absorber structure.

II. Equivalent Circuit Model

The metamaterial absorber under consideration consists of an array of square-shaped ring structure and grounded dielectric substrate as shown in Fig. 1(a). FR-4 substrate has been used as dielectric ($\varepsilon_r = 4.25$ and $tan\delta = 0.02$) with 1 mm thickness, whereas both the top metallic patch and bottom ground are made of copper (conductivity $\sigma = 5.8 \times 10^7$ S/m), each having thickness of 0.035 mm.

When a plane wave is normally incident on the structure, the electric field is distributed in such a way that the surface currents in the FSSs form a closed loop as shown in Fig. 2. According to

Manuscript received June 21, 2014; revised September 20, 2014; accepted November 05, 2014. Date of publication November 12, 2014; date of current version February 06, 2015. This work was supported in part by DRDO, India, under Project No. DLJ/TC/1025/I/30 and ISRO-IITK Space Technology Cell under Project No. STC/EE/2014087.

The authors are with the Department of Electrical Engineering, Indian Institute of Technology Kanpur, Kanpur 208016, India (e-mail: joysaptarshi@gmail.com; kvs@iitk.ac.in).

Color versions of one or more of the figures in this letter are available online at http://ieeexplore.ieee.org.

Digital Object Identifier 10.1109/LAWP.2014.2369732

1536-1225 © 2014 IEEE. Personal use is permitted, but republication/redistribution requires IEEE permission.
See http://www.ieee.org/publications_standards/publications/rights/index.html for more information.

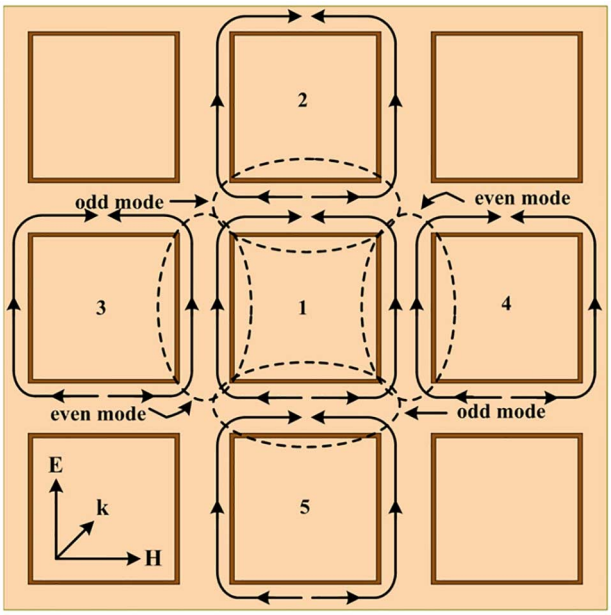

Fig. 2. Even- and odd-mode couplings in the proposed structure.

the surface current directions in the array structure, each square loop (1) is coupled with the neighboring unit cells through even- (3, 4) and odd-mode (2, 5) coupling [11].

Fig. 1(b) shows the construction of the equivalent circuit model, which comprises a parallel connection of FSS impedance and grounded reactance. The FSS impedance, consisting of series resonators, can be expressed as

$$Z_{\mathrm{FSS}} = R_{\mathrm{FSS}} + j\omega L_{\mathrm{FSS}} + 1/j\omega C_{\mathrm{FSS}} \tag{1}$$

where L_{FSS} is the FSS inductance corresponding to the length (l) of the square ring and C_{FSS} is the FSS capacitance between two adjacent unit cells. R_{FSS} is the resistance of the top copper patch, which has been modeled due to finite conductivity of the copper metal. On the contrary, the substrate impedance can be expressed as

$$Z_{\mathrm{TML}} = Z_{\mathrm{d}} + Z_{\mathrm{C}} = j\sqrt{(\mu_0\mu_{\mathrm{r}})/(\varepsilon_0\varepsilon_{\mathrm{r}})}\tan(kd) + R_{\mathrm{d}} + 1/j\omega C_{\mathrm{C}} \tag{2}$$

where ε_{r} and μ_{r} are the electric permittivity and magnetic permeability of the grounded dielectric substrate, respectively. $k = k_0\sqrt{\varepsilon_{\mathrm{r}}\mu_{\mathrm{r}}}$ is the wavenumber of the incident wave in the substrate. R_{d} is the equivalent resistance due to dielectric loss in the substrate representing the imaginary part of the material parameters, and C_{C} is the coupling capacitance due to periodic structure [11].

For an independent unit cell, the (top surface) FSS impedance comes in parallel with the grounded short-circuited transmission line, which shows an inductive behavior [9]. However, when the metallic patches are arranged in periodic array, there is an extra coupling capacitance that can be calculated based on coupled-line geometry of the microstrip line. The even-mode coupling (between 1 and 3, 1 and 4) provides only the vertical coupling capacitance, whereas the odd-mode coupling (between 1 and 2, 1 and 5) produces both the vertical and horizontal coupling capacitances [11]. Here, C_{FSS} has been designated as the horizontal coupling capacitance between the adjacent unit cells, while C_{C} has been used to describe the vertical coupling capacitance between the FSS and the ground plane.

Therefore, the surface impedance Z_{S} can be viewed as the parallel combination between Z_{FSS} and Z_{TML}, expressed as

$$Z_{\mathrm{S}} = Z_{\mathrm{FSS}} \| Z_{\mathrm{TML}}. \tag{3}$$

Since the equivalent circuit behaves as a parallel RLC circuit, at resonance frequency the real part of Z_{S} will match closely with the free-space impedance (η_0), and the imaginary part will tend to infinity [8], [12]. By resorting to the theory of microstrip lines, the effective permittivity ($\varepsilon_{\mathrm{re}}$) and characteristic impedance (Z_{C}) for the homogenous dielectric material can be calculated from [13] for the given strip width (w) and dielectric thickness (d). Then, using quasi-static analysis of microstrip line, the inductance per unit length is obtained as $L = \frac{Z_{\mathrm{C}} \times \sqrt{\varepsilon_{\mathrm{re}}}}{c}$, which gives rise to the FSS inductance (L_{FSS}) by multiplying with the requisite patch length. On the other hand, even- and odd-mode excitation of the structure gives rise to the coupling capacitance C_{C} and FSS capacitance C_{FSS} [11]. The right-angle bending parts of the square-shaped structure provide some extra inductive and capacitive effects, which have also been incorporated by calculating them through some empirical formulas [13].

III. Numerical Results

The absorption frequency can be obtained from (1)–(3) by considering the reactance part of surface impedance Z_{S} to infinity. The calculated values for the lumped elements are as follows: $C_{\mathrm{FSS}} = 171.55$ (fF), $C_{\mathrm{C}} = 280.08$ (fF), and $L_{\mathrm{FSS}} = 5.05$ (nH) corresponding to the absorber structure having unit cell width $(w) = 0.2$ mm, length $(l) = 7.5$ mm, period $(a) = 10$ mm, and substrate thickness $(d) = 1$ mm. These values lead to the absorption frequency calculated as 6.14 GHz, whereas full-wave simulation (by ANSYS HFSS) of the absorber structure results to 6.13 GHz. The exact matching between the responses clearly validates the modelization technique for the absorber structure.

Since the absorption frequency as well as the FSS inductance (L_{FSS}), FSS capacitance (C_{FSS}), and coupling capacitance (C_{C}) are primarily related to the width of the unit cell (w), length of the square loop (l), permittivity ($\varepsilon_{\mathrm{re}}$), and thickness of the dielectric substrate and period of the square ring (a), the variations of these parameters are investigated in Fig. 3. As width (w) of the square ring increases, L_{FSS} decreases and C_{C} increases, while the absorption frequency increases slowly. All the three lumped elements L_{FSS}, C_{FSS}, and C_{C} increase and the absorption frequency decreases with the length (l) of the unit cell. Both C_{FSS} and C_{C} gradually increase with increasing $\varepsilon_{\mathrm{re}}$, while L_{FSS} remains constant; this decreases the absorption frequency with increase of dielectric permittivity of the substrate. When the thickness of the substrate (d) is increased, C_{FSS} remains almost constant, C_{C} decreases, L_{FSS} increases, and the absorption frequency reduces slowly. Finally, as the unit cell period (a) increases, keeping length of the unit cell (l) to be constant, the frequency of absorption increases up to a certain limit and thereafter remains constant. In all the cases, the numerical results match closely the simulated responses. Since some of the impedance expressions used in the model are derived empirically [11], [13], [14], small deviations are observed in all the five cases, although within acceptable limit.

To understand the absorption mechanism, C_{FSS}, C_{C}, and L_{FSS} of the square ring are analyzed for different values of

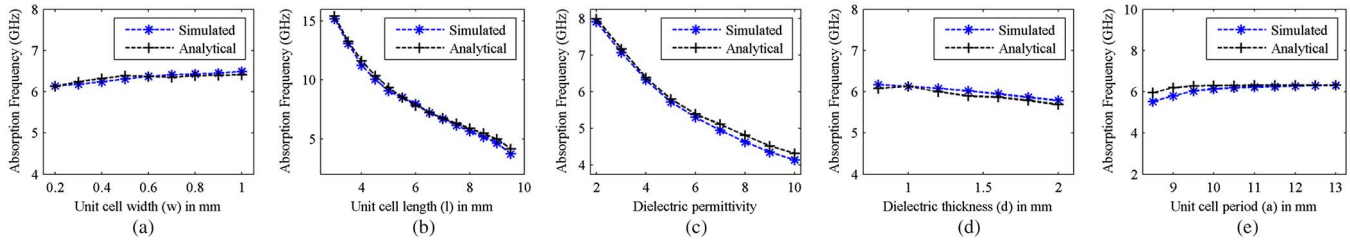

Fig. 3. Comparison of analytical and simulated absorption frequencies for different (a) widths of the square ring, (b) lengths of the square ring, (c) dielectric permittivities, (d) thicknesses of the substrate, and (e) unit cell periods of the structure.

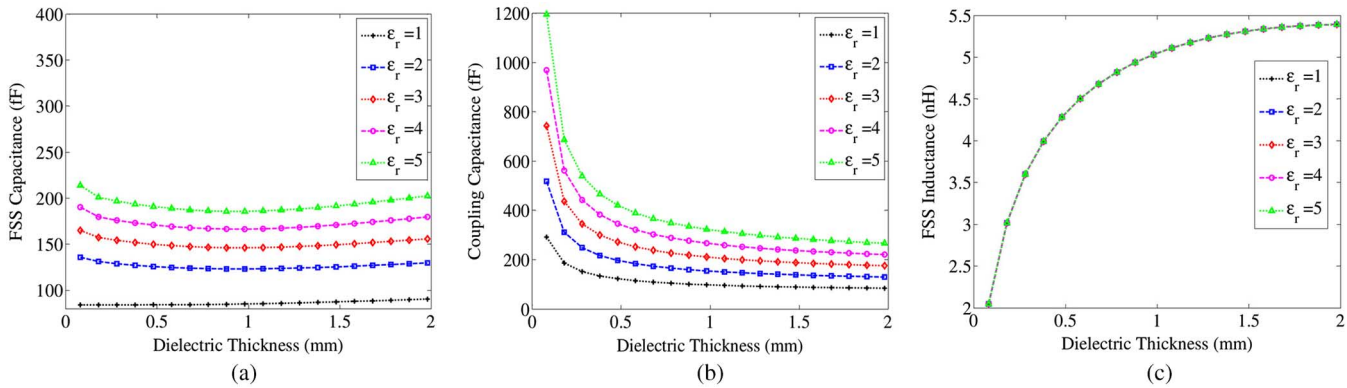

Fig. 4. Variation of (a) FSS capacitance, (b) coupling capacitance, and (c) FSS inductance for different substrate thicknesses with different values of permittivity.

dielectric permittivity as a function of substrate thickness in Fig. 4. C_{FSS} remains almost constant with the dielectric thickness value, as it mainly depends on the surface charge distribution. Coupling capacitance C_{C}, starting from very high value near ground plane, approaches to some finite constant with increasing the substrate thickness, whereas L_{FSS} increases nonlinearly with thickness showing in the same way as in the case of microstrip line theory [15]. Although C_{FSS} and C_{C} increase linearly with permittivity, L_{FSS} remains constant during variation of the permittivity of the dielectric substrate. Since the characteristic impedance Z_{C} is inversely proportional to $\sqrt{\varepsilon_{\mathrm{re}}}$ (for microstrip line), the overall term ($L = Z_{\mathrm{C}} \times \sqrt{\varepsilon_{\mathrm{re}}}/c$) is independent of the effective permittivity of the substrate [13].

The effects of dielectric permittivity and substrate thickness on FWHM bandwidth of the absorber structure have been investigated based on the analytical method presented here. As shown in Fig. 5(a), the FWHM bandwidth of the metamaterial absorber increases almost linearly with the substrate thickness [16]. On the other hand, as $tan\delta(= \varepsilon''/\varepsilon')$ remains constant, with increasing real part of dielectric constant (ε'), its imaginary part (ε'') decreases, which increases quality factor and reduces the FWHM bandwidth as shown in Fig. 5(b). Since both the resistances R_{FSS} and R_{d} are unknown, some constant values have been considered for calculating the FWHM bandwidth, which leads to the deviation between the calculated and simulated responses. However, the pattern remains similar, thus supporting the results due to variation.

The proposed structure has been fabricated on 1-mm-thick FR-4 substrate using standard printed circuit board (PCB) technology as shown in Fig. 6(a). The structure has been measured in an anechoic chamber using standard gain horn antennas (C-band) and a network analyzer (Agilent N5230A). Fig. 6(b) shows the simulated, measured, and calculated

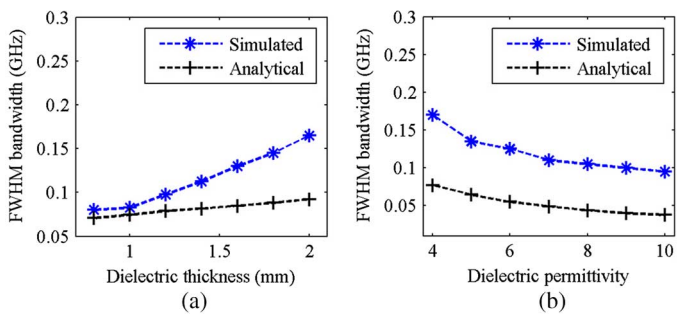

Fig. 5. Comparison of FWHM bandwidth for (a) different substrate thicknesses and (b) different dielectric permittivities of the structure.

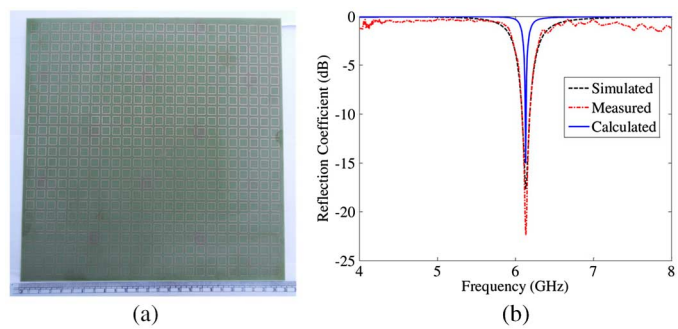

Fig. 6. (a) Photograph of the fabricated absorber, and (b) comparison among simulated, measured, and calculated reflection coefficient of the structure.

reflection coefficients (S_{11}) of the proposed structure, which are in good agreement, thus validating the analytical model. The small deviation of the peak absorptivity and absorption

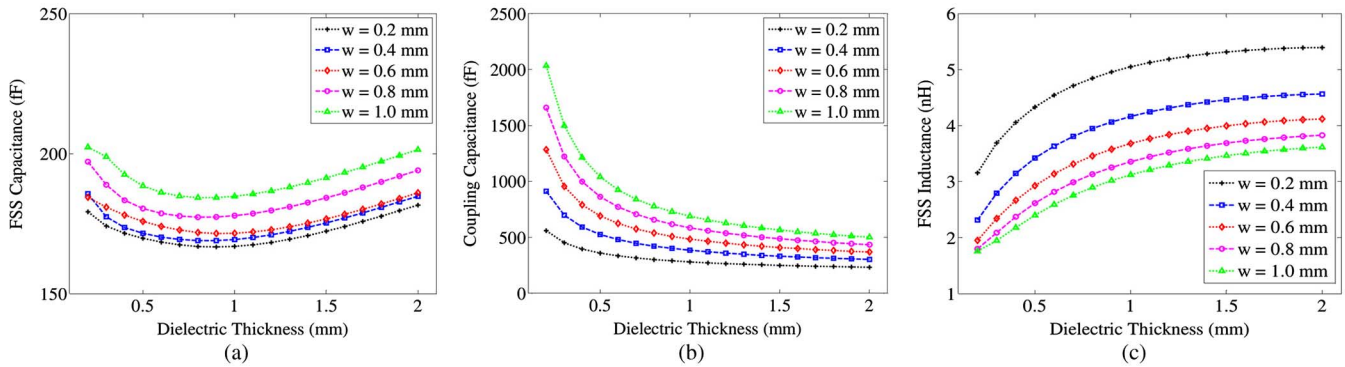

Fig. 7. Variation of (a) FSS capacitance, (b) coupling capacitance, and (c) FSS inductance for different widths with different substrate thicknesses.

bandwidth may be due to the deviation of ohmic and dielectric resistances ($R_{\rm d}$ and $R_{\rm FSS}$) from their ideal values.

Although the equivalent circuit model of other geometries (like circular ring, patch, cross, etc.) are not discussed here for sake of brevity, their absorption frequencies can also be calculated through this technique. To get a glimpse about the nature of variation of different lumped elements with the width of the square ring, the substrate thickness of the structure has been varied, keeping the permittivity constant. The FSS capacitance ($C_{\rm FSS}$), coupling capacitance ($C_{\rm C}$), and FSS inductance ($L_{\rm FSS}$) curves are mentioned in Fig. 7. It can be noticed that by increasing the percentage of metal in the FSS unit cell, the FSS capacitance ($C_{\rm FSS}$) gradually increases, whereas the FSS inductance ($L_{\rm FSS}$) decreases. On the contrary, the deviation of coupling capacitance ($C_{\rm C}$) among the FSSs having different widths at low substrate thickness is very high and gradually approaches to constant value while increasing the thickness. Therefore, we can finally conclude that by properly synthesizing the lumped element values, the equivalent circuit model can be employed for analyzing metamaterial absorber structure based on FSSs.

The above calculation has been done considering normal incidence plane wave. Since the proposed equivalent circuit model is based on the surface current distribution, it can also be applied for various oblique incidence and polarization angles. In case of oblique incidence, there will be always a component of electromagnetic field along initial direction (except for 90° incidence), thus satisfying the same current flow. The only change will be in the electrical path length of the wave traversed through the dielectric, which will cause a slight shift in absorption frequency. In case of polarization angle variation, absorption frequency will remain constant (except for 90° polarization) as long as there is a component of wave along the initial direction.

IV. Conclusion

In this letter, a simple equivalent circuit model based on transmission line and even/odd-mode coupling theory is presented to accurately design any metamaterial absorber structure comprising arbitrary shaped FSS. A single square ring (exhibiting a narrow frequency band) with grounded dielectric substrate has been used as an absorber structure to explain the analytical model. Other FSS elements like cross, patch, rings, dual-/multiband geometries, etc., can also be modeled though this technique as long as their surface current flows are known and intra/intercouplings can be calculated. The dimensions of the unit-cell FSS are related to the parallel RLC circuits, and their effects on the absorption frequency have been investigated. The variations of substrate thickness and dielectric permittivity have been studied for optimizing the FWHM bandwidth. The calculated result matches well with the simulated and measured responses with minor deviation. The proposed equivalent circuit can be considered as a generalized model for analyzing absorber structures of arbitrary shaped frequency selective surfaces.

References

[1] B. A. Munk, *Frequency Selective Surfaces—Theory and Design*. New York, NY, USA: Wiley, 2000.
[2] O. Luukkonen, F. Costa, C. R. Simovski, A. Monorchio, and S. A. Tretyakov, "A thin electromagnetic absorber for wide incidence angles and both polarizations," *IEEE Trans. Antennas Propag.*, vol. 57, no. 10, pp. 3119–3125, Oct. 2009.
[3] F. Costa, A. Monorchio, S. Talarico, and F. M. Valeri, "An active high impedance surface for low profile tunable and steerable antennas," *IEEE Antennas Wireless Propag. Lett.*, vol. 7, pp. 676–680, 2008.
[4] C. C. Chen, "Transmission through a conductive screen perforated periodically with apertures," *IEEE Trans. Microw. Theory Tech.*, vol. MTT-18, no. 9, pp. 627–632, Sep. 1970.
[5] R. Mittra, C. H. Chan, and T. Cwik, "Techniques for analyzing frequency selective surfaces- a review," *Proc. IEEE*, vol. 76, no. 12, pp. 1593–1615, Dec. 1988.
[6] R. J. Langley and E. A. Parker, "Equivalent circuit model for arrays of square loops," *Electron. Lett.*, vol. 18, no. 7, pp. 294–296, 1982.
[7] H. X. Xu *et al.*, "Triple-band polarization-insensitive wide-angle ultraminiature metamaterial transmission absorber," *Phys. Rev. B*, vol. 86, p. 205104, 2012.
[8] F. Costa, S. Genovesi, and A. Monorchio, "On the bandwidth of high-impedance frequency selective surfaces," *IEEE Antennas Wireless Propag. Lett.*, vol. 8, pp. 1341–1344, 2009.
[9] Y. Pang, H. Cheng, Y. Zhou, and J. Wang, "Analysis and design of wire-based metamaterial absorbers using equivalent circuit approach," *J. Appl. Phys.*, vol. 113, p. 114902, 2013.
[10] S. Ghosh, S. Bhattacharyya, Y. Kaiprath, and K. V. Srivastava, "Bandwidth-enhanced polarization-insensitive microwave metamaterial absorber and its equivalent circuit model," *J. Appl. Phys.*, vol. 115, no. 10, p. 104503, 2014.
[11] R. Garg and I. J. Bahl, "Characteristics of coupled microstriplines," *IEEE Trans. Microw. Theory Tech.*, vol. MTT-27, no. 7, pp. 700–705, Jul. 1979.
[12] Y. Pang, H. Cheng, Y. Zhou, and J. Wang, "Upper bound for the bandwidth of ultrathin absorbers comprising high impedance surfaces," *IEEE Antennas Wireless Propag. Lett.*, vol. 11, pp. 224–227, 2012.
[13] J. S. Hong and M. J. Lancaster, *Microstrip Filters for RF/Microwave Applications*, 2nd ed. New York, NY, USA: Wiley, 2001, pp. 85–92.
[14] K. C. Gupta, R. Garg, I. Bahl, and P. Bhartia, *Microstrip Lines and Slotlines*, 2nd ed. Boston, MA, USA: Artech House, 1996, pp. 179–196.
[15] F. Costa, A. Monorchio, and G. Manara, "An equivalent-circuit modeling of high impedance surfaces employing arbitrarily shaped FSS," in *Proc. ICEEA*, Turin, Italy, Sep. 2009, pp. 852–855.
[16] R. Huang, "Ultrathin metamaterial screens with nonuniform patches for reflectivity reduction from metallic surfaces," *IEEE Trans. Magn.*, vol. 49, no. 5, pp. 2157–2160, May 2013.